Biomaterials 290 (2022) 121820

Contents lists available at ScienceDirect

Biomaterials

journal homepage: www.elsevier.com/locate/biomaterials

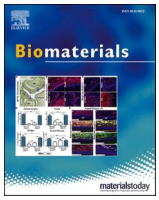

In vivo therapeutic effects of small molecule-drug conjugates enhanced by Fc grafting

Yan Zheng [a], Ruolin Xu [a], Siyi Chen [a], Wanyi Tai [a,b,c,*]

[a] Department of Pharmacy, Zhongnan Hospital of Wuhan University, School of Pharmaceutical Sciences, Wuhan University, Wuhan, Hubei, 430071, China
[b] Cancer Precision Diagnosis and Treatment and Translational Medicine Hubei Engineering Research Center, Zhongnan Hospital of Wuhan University, Wuhan, Hubei, 430071, China
[c] Wuhan Research Center for Infectious Diseases and Cancer, Chinese Academy of Medical Sciences, Wuhan, Hubei, 430071, China

ARTICLE INFO

Keywords:
Small-molecule ligand
Antibody drug conjugate
Fc grafting
Targeted delivery
Cancer therapy

ABSTRACT

Small molecule-drug conjugate (SMDC) shows great potential as a new class of targeted chemotherapeutic agents to tackle cancer. However, its in vivo therapeutic effect is compromised by its poor pharmacokinetic parameters. Herein we describe an approach that enables the precise conjugation of SMDC on N-terminus of the Fc protein to produce a SMDC-Fc bioconjugate (Fc1070) with superior specificity, affinity and potency to tumor cells. In vivo, Fc1070 exhibited an antibody-like pharmacokinetic profile with a long circulation half-life (t1/2 = 79 h) and pro-liver clearance pathway, that is distinct from the parent SMDC (t1/2 = 0.5 h and renal clearance). Intravenous injection of Fc1070 can eliminate the tumor with a single dosing of 7 mg/kg. Coupled with a predefined ligand toolbox, this approach allows the fast generation of other SMDC bioconjugates on demand, thus extending the format easily to other tumor targets. This may provide a general approach for the development of SMDC with enhanced therapeutic properties.

1. Introduction

Targeted chemotherapy has been emerging as a promising modality of treatment for cancer patients, especially for those that have refractory forms or show resistance to other treatments. In contrast to the standard chemotherapy that destroys both cancer and healthy cells, targeted chemotherapeutic agents utilize a tumor-specific ligand to preferentially localize and act at the tumor site, thus increasing the effectiveness of applied dose and reducing the systemic toxicity. To date, both monoclonal antibodies and small-molecule ligands have been widely explored as tumor homing ligands for drug conjugation and targeted chemotherapy [1]. The former, comprised of highly potent drugs chemically conjugated to a full-length antibody, also known as antibody-drug conjugate (ADC), has achieved numerous clinical success, with approval of 12 ADCs in oncological therapy [2]. Bolstered by the success of ADC, small molecule-drug conjugate (SMDC), the later that use small organic compound as ligand, has gain the growing interest as well [3–5].

Despites much smaller size, SMDC can achieve the nanomolar to picomolar affinity to its target without compromise in the specificity and selectivity of binding [6]. Some small-molecule ligands, such as folic acid and DUPA, are derived from the targets' cognate ligands, which would have inherent good safety and immunotolerance. The simplicity in structure also confers several important advantages in the context of deep tumor penetration and cheap manufacturing cost, both of which have been extensively discussed elsewhere [7]. In spite of the attractive features as aforementioned, SMDC has the pharmacokinetic limitation, in brief the extremely short half-life in circulation, which would prevent the gradual accumulation of drugs in tumor and in turn limit its therapeutic efficacy [7]. ADC, on the other hand embracing long blood retention and high tumor uptake, however is far more complex in structure and costly in production, reflecting the need of expensive antibody manufacturing and design per drug for conjugating [8,9].

The long plasma half-life of ADC is preserved from its antibody component. Technically speaking, the Fragment Crystallizable (Fc) domain that mediates the Fc receptor (FcRn) recycling process, is the proposed origin of this unique property [10,11]. It has been demonstrated that Fc grafting, mainly by genetic fusion, can elongate the half-life of a payload in blood circulation dramatically [12]. This notion proves to be a broadly applicable strategy and has already bolstered the clinical success of enormous Fc-fusion proteins and Fc fusion peptides,

* Corresponding author. Department of Pharmacy, Zhongnan Hospital of Wuhan University, School of Pharmaceutical Sciences, Wuhan University, Wuhan, Hubei, 430071, China.
E-mail address: wanyi-tai@whu.edu.cn (W. Tai).

https://doi.org/10.1016/j.biomaterials.2022.121820
Received 23 June 2022; Received in revised form 2 September 2022; Accepted 20 September 2022
Available online 24 September 2022

for example Etanercept, Abatacept and Dulaglutide [13]. Motivated by the eminent effect of Fc on half-life extension, it has been recently programed to graft with SMDC by Gallo et al. [14]. However, this Fc-SMDC scaffold displayed a biphasic pharmacokinetic profile in mice with a quick elimination of the majority of dose from body in the first phase ($t1/2 = 26$ min). The suboptimal pharmacokinetics of Fc-SMDC is likely attributed to the C-terminal grafting strategy in which SMDC was conjugated to the C-terminus of Fc, while controversially the clinically approved Fc fusion protein (also ADC) leaves C-terminus free and linked with exogenous payloads through N-terminus.

The pilot study by Gallo et al. and the very encouraging development in the field of Fc fusion proteins motivated us to focus on the possibility to graft SMDC with N-terminus for better in vivo performance. Here, we reported the development of a SMDC-Fc bioconjugate that is composed by small-molecule ligand, drug and Fc protein. The SMDC-Fc platform was constructed by enzymatically extending the N-terminus of a human IgG Fc with cytotoxic drug MMAF and subsequently installing a tumor-homing ligand by click reaction (Scheme 1). The key intermediate MMAF-Fc fusion protein acts as a 'one-piece-fits-all' module and readily integrates with a 'click-and-go' ligand toolbox to generate a collection of Fc bioconjugates in the high throughput manner. By traceless ligation of drug at N-terminus, the scaffold well preserves the main peptide chains of Fc and was expected to exhibit a maximal biological performance in mice. We speculated that this on-demand construct can significantly enhance biological half-life with a concomitant increase of drug delivery efficiency to the tumor while maintaining a compact size and stable scaffold. Because of the easy expression of Fc protein in *E. Coli* and feasible access to synthetic ligands [15], this platform also affords the unique opportunity for the massive production of targeted chemotherapeutic agents at low cost.

2. Results and discussion

2.1. Design and characterization of SMDC-Fc bioconjugate

Monomethyl auristatin F (MMAF) is an antimitotic pseudopeptide that has showed great success as a toxin in ADC development [16]. MMAF was chose from a bunch of ADC toxins in this study because of its peptide-like structure and free-carboxyl C-terminus. This feature allows us to treat it as a short peptide and tracelessly fuse to the Fc's N-terminus to yield a MMAF-Fc fusion protein. Despites mingled with a small handful of non-natural amino acids (e.g., Mov, Dil, Dap from MMAF), the MMAF-Fc fusion protein maintains intact N-to-C peptide chains and keeps all the residues unmodified. Moreover, the drug MMAF locates at the distal end from Fc domain and serves as an extra extension of the hinge region. All of the features help to mitigate the heterogeneity and instability caused by drug integration, therefore maximizing the biological performance.

Controversy to the hallmark of linker attachment to the N-terminal monomethylvaline (Mov) of MMAF [17], in this study we used the C-terminal carboxyl group as a point of linker attachment in order to preserve the chain's sequence orientation. Since the drug's C-terminal residue (Phe) together with the appended azido lysine (Azl) would be linked with chemical ligand, it was expected that the linker sequence LPETGG would dictate the repertoire of proteolytic drug release, and would also modulate the Sortase A-mediated drug ligation to Fc protein (Scheme 1). Assembly of drug and antibody using sortase ligation proved more amenable to the precise control of drug-to-antibody ratio (DAR) than conventional chemical methods, especially since site-specific conjugation to N-terminus is requisite in this study [18,19]. Moreover, the amide linker, peptide bond generated by transpeptidation, is expected to be more stable than the thioester/maleimide method [20,21].

To increase the ligation efficiency, a depsipeptide (peptide bond between Thr and Gly is replaced by an ester bond) was added to the

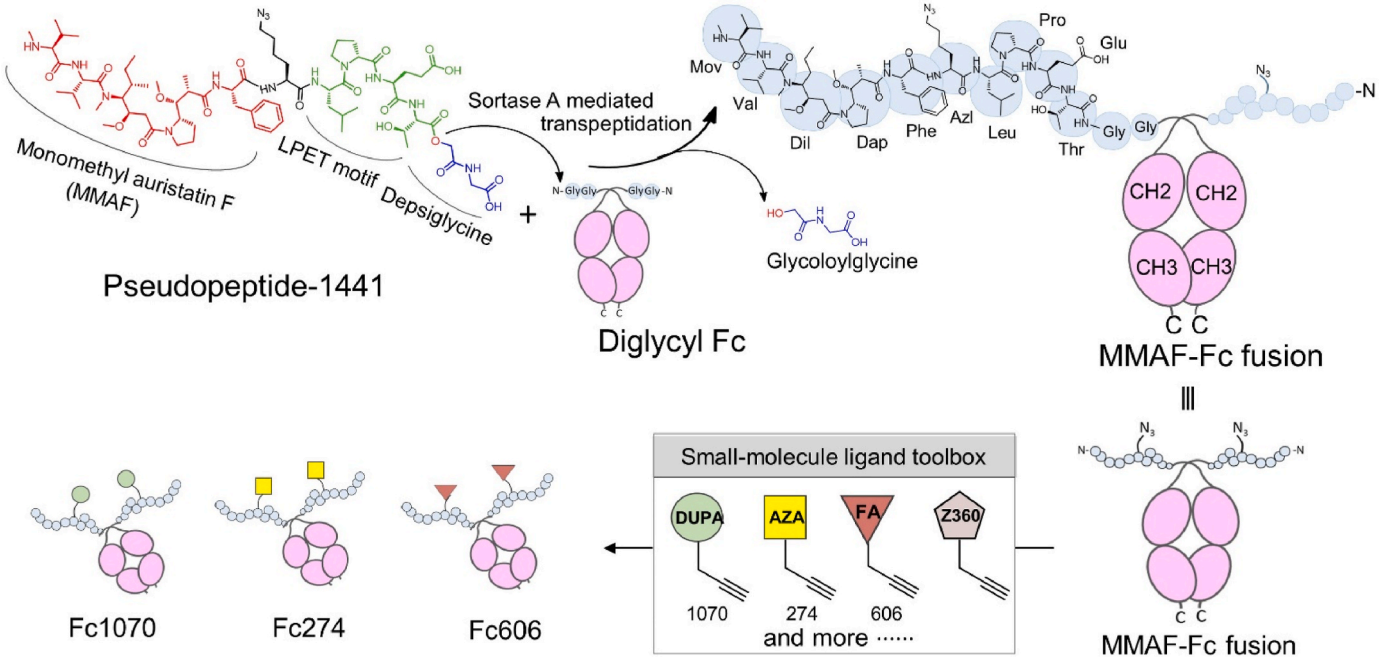

Scheme 1. Schematic representation of SMDC-Fc construction process. Pseudopeptide-1441 bearing MMAF and depsipeptide substrate was site-specifically incorporated to the N-terminus of the Fc protein by Sortase A-mediated transpeptidation. By utilizing the Cu(I)-catalyzed click reaction, the tumor-homing small-molecule ligands were installed on the azido "handler" of MMAF-Fc fusion protein to yield the SMDC-Fc on demand, e.g., the PSMA targeting SMDC-Fc Fc1070. MMAF-Fc fusion protein served as a 'one-piece-fit-all' module and can be readily conjugated with a diverse set of ligands from toolbox to create the paradigm for broad utility. The DUPA, AZA, FA and Z360 are the names of small-molecule ligands that target to PSMA, CAIX, FR and CCK2R receptors, respectively. The numbers indicate their molecular weight.

LPET motif tail to render the ligation reaction irreversible [22]. The key intermediate pseudopeptide-1441 is composed of three components: MMAF, LPET motif and depsiglycine. It was synthesized by adduction of depsiglycine and MMAF to the LPET motif in order, as shown in Scheme 2. During ligation, it can be readily recognized by Sortase A enzyme and site-specifically transferred to the N-terminus of the diglycyl Fc protein. The N-terminal diglycine is an essential sequence for sortase A recognition. Its preparation method and characterization are available in Fig. S1. To guarantee the fusion protein with a defined DAR of 2, we set out to optimize the ligation condition by titrating the molar ratio of pseudopeptide-1441 and Fc protein. As monitored in the hydrophobic interaction chromatography (HIC) of Fig. 1A, the desired product of DAR ≈2, was obtained by using typically 10 molar equivalents of pseudopeptide-1441 per molar equivalent of Fc protein in the presence of 0.05 molar equivalent of Sortase A. Addition of less pseudopeptide-1441 or more Sortase A would result in lower DAR ratio, likely due to insufficient competition or reverse hydrolysis by the enzyme. This condition was also confirmed by monitoring the ligation progress with SDS-PAGE under reducing condition (Fig. S2A). Meanwhile, a size exclusion chromatography (SEC) experiment coupled to nonreducing SDS-PAGE analysis was performed to confirm that the MMAF-Fc fusion protein retained its disulfide-linked homodimer state after ligation (Fig. 1B and S2C).

To this step, we have obtained the MMAF-Fc fusion protein bearing two molecules of drugs and azido groups by fusing a piece of pseudopeptide to the Fc's N-termini. Utilizing the click reaction, this fusion protein would act as the 'one-piece-fits-all' module to construct a diverse-set of SMDC-Fc on demand. To simplify the development process, we established a small-molecule ligand toolbox which so far contains only 4 members but can be expanded as needed in future. Each of these ligands encompasses a tumor-homing chemical ligand and an alkyne group on other end for click chemistry. After copper-catalyzed alkyne–azide 1,3-dipolar cycloaddition (CuAAC), the reaction was simply desalted and can be directly evaluated for the biological activities without the need of any further manipulation.

Focusing on prostate cancer therapy, we first constructed a SMDC-Fc (Fc1070) targeting prostate specific membrane antigen (PSMA) using the ligand DUPA-1070 [23,24]. We performed ESI-TOF mass analysis under reducing condition to trace each step of the construction process (Fig. 1C). As for the diglycyl Fc, the deconvolution results exactly matched the calculated mass of the defined heavy chain. In parallel, MMAF-Fc fusion protein was detected at two masses of 26480 (dwarf peak) and 27789 Da (main peak), which could be assigned to the Fc chains without or with MMAF ligated, respectively. Integration of the mass peak areas result in an average DAR of 1.90, which is comparable to the result observed by HIC (DAR = 1.95). After the ligand installation via click reaction, the *m/z*m/z of Fc1070 shifted toward higher mass, resulting in a main mass peak of 28858 Da. The mass difference of 1069 Da perfectly matched with the relative molecular weight of ligand DUAP-1070 from the toolbox, thus suggesting that Fc1070 was successfully equipped with the PSMA specific ligand. Two diminutive peaks of 26480, 27789 Da were also observed in the deconvoluted mass spectrum of Fc1070, suggestive for the presence of negligible amount of unreacted proteins. The purity and molecular weight of the products were further confirmed by SDS-PAGE, showing the band migration to higher molecular weight after each labeling reaction (Fig. 1B and Fig. S2B). Only a single band was observed in each reaction, indicating the predominance of the programmed products.

2.2. Selectivity and potency toward tumor cells

Initial evaluation of Fc1070 was carried out in three human prostate cell lines, selected based on their PSMA status: LNCaP ($PSMA^{++}$), 22RV1 ($PSMA^{+}$) and PC-3 ($PSMA^{-}$) [25]. For quantitative analysis of the selectivity using flow cytometry, the N-terminal monomethyl amine of MMAF was fluorescently labelled with sulfo-Cy5. A number of results were presented in Fig. 2A. First, the binding of Fc1070 on LNCaP cells is dose-dependent. With concentration of 5 nM of Fc1070 or higher, a large shift in fluorescence intensity was observed on LNCaP cells in comparison to the blank control. To further confirm the selectivity of binding, an inhibition assay was conducted utilizing a well-established PSMA inhibitor, 2-(phosphonomethyl)-pentanedioic acid (PMPA), that shares the same binding pocket with the small-molecule ligand DUPA [26]. The fluorescent signal of Fc1070 on LNCaP cells can be reduced to nearly the background level by 1000 nM of PMPA, confirming the specificity of Fc1070 to PSMA receptor. In parallel with the inhibitory experiment, we compared the binding capability of Fc1070 on all three prostate cell lines. Fc1070 can effectively bind to both LNCaP and 22RV1 cells but not the PC-3 cells. Meanwhile, the mean fluorescent intensity on LNCaP cells is slightly higher than that of 22RV1, which is in correlation with the levels of their PSMA expression.

In the flow cytometry analysis, we noticed that Fc1070 always showed higher binding capability than its counterpart SMDC1070 on PSMA-positive cell lines (both LNCaP and 22RV1). Considering the share of same targeting ligands, the enhanced binding activity is likely due to the bivalent characteristic of Fc1070. Homodimerization of Fc chains positions two small-molecule ligands parallel to form a dimer that can increase the apparent affinity of Fc1070 to PSMA receptors, a phenomenon similar to the antibody bivalency [27]. To further evaluate the bivalent effect of Fc1070, the dissociation constant (KD) of Fc1070 to PSMA receptor was measured and compared with SMDC1070 using the MicroScale Thermophoresis (MST) assay (Fig. 2B and C). Gradient titration of Fc1070 against 10 nM of PSMA receptor (fusion with fluorescent protein mClover) yielded a KD of 7.8 ± 2.1 nM, which is roughly 3 times lower than that of SMDC1070 (KD = 24 ± 7.1 nM), rendering Fc1070 a much stronger high-affinity binder.

The strong affinity prompted us to test the bioactivity on prostate cancer cell lines, as showed in Fig. 2E. PSMA positive LNCaP cells were exposed to Fc1070 continuously for 72 h, and the cytotoxic effects, as determined by CCK8 viability assay, were compared to the precursors MMAF-Fc and diglycyl Fc (Fig. 2E, left panel). On a molar basis, Fc1070 (IC50 = 1.8 ± 0.6 nM) was at least 500-fold more potent than the ligand-free MMAF-Fc (IC50 > 1000 nM). This SMDC-Fc was also active on another PSMA positive 22RV1 cells, despites showing a lower activity (Ic50 = 13 ± 4 nM). Apparently, the cytotoxic effects were cell-type specific, since another cell line PC-3, which does not express PSMA receptors at all, were unaffected by the Fc1070 (Fig. 2E, middle left). Further studies with SMDC1070 and MMAF were undertaken on LNCaP cells and compared to Fc1070. LNCaP was quite sensitive to both SMDC1070 and Fc1070, while it was less affected by MMAF (Fig. 2E, middle right). This trend strengthens the previous assumption that MMAF is cell membrane-impermeable and requires ligand-mediated internalization for activity. Surprisingly, SMDC1070, a weaker binder as stated earlier and just carrying one drug per molecule in comparison to two in Fc conjugate, was more potent than Fc1070. Further profiling the cytotoxicity against drug-treatment time revealed that SMDC1070 exhibit a faster rate of cytotoxicity, as the onset of toxicity was observed imminently after feeding SMDC1070, while the growth profile of cells treated by Fc1070 displayed an inverted J curve, indicating that the cell proliferation was not interrupted at the initial stage (roughly one-day delay). As a result, the half (50%) cell viability was achieved by 1.5 days after adding SMDC1070, in comparison to 2.4 days by Fc1070 (Fig. 2E, right panel). The delay of activity might be imputed to the necessity of Fc proteolysis for the drug release and cytotoxicity. This hypothesis was exemplified by the benchmark ADC Trastuzumab-MCC-DM1 (T-DM1), which was found to hydrolyze into the active form lysine-MCC-DM1 in lysosome after receptor-mediated internalization [28]. In light of these studies, it was safe to postulate that Fc1070 would undergo the proteolytic degradation of Fc domain in the lysosome of tumor cells and release the active metabolites, likely a SMDC, as the major cell-killing agent.

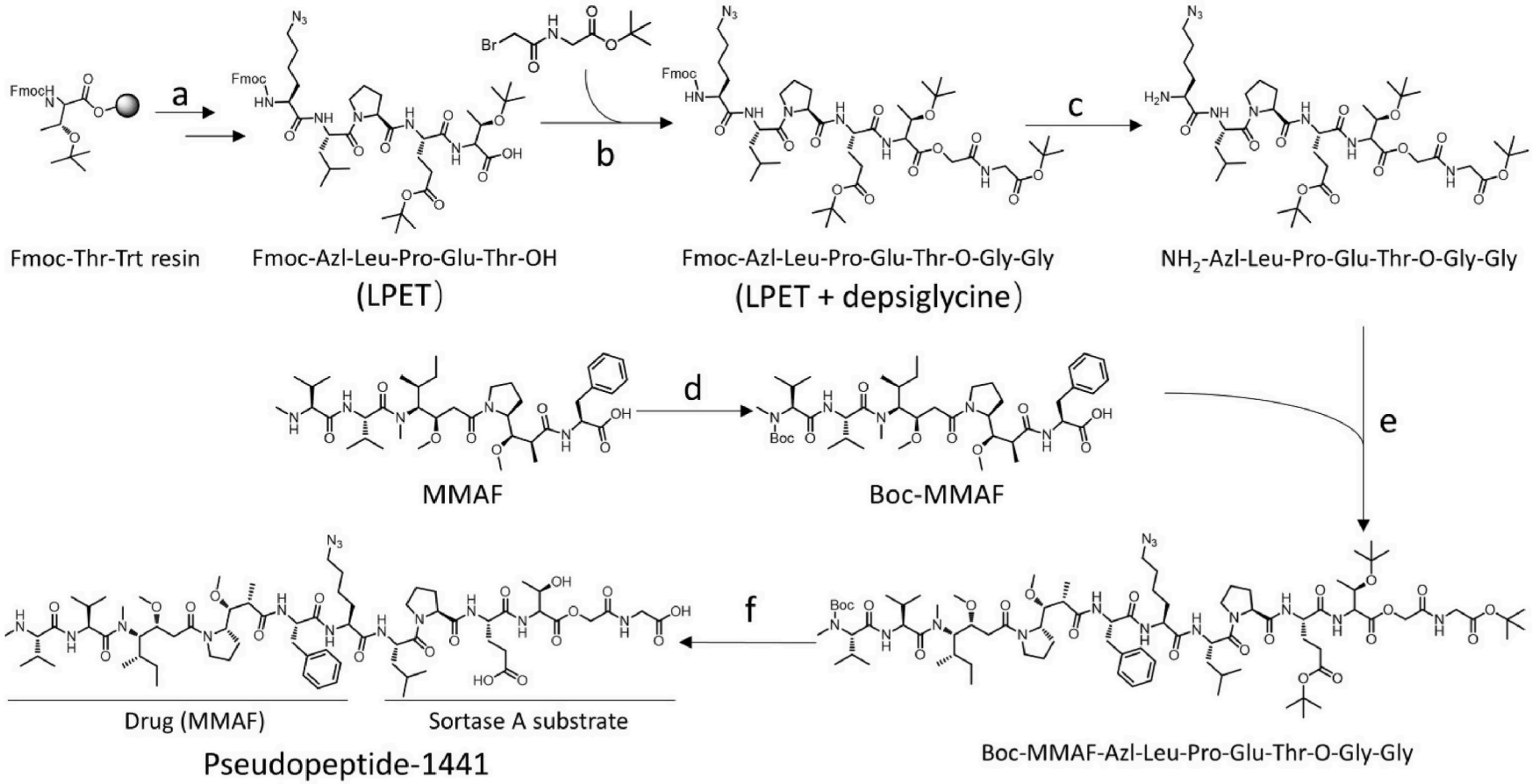

Scheme 2. Synthesis of pseudopeptide-1441. (a) i. Fmoc-AA-OH, HATU, DIPEA, DMF; ii. 20% piperidine, DMF; iii. 10% AcOH, DCM, TFE; (b) DIPEA, TBAI, THF; (c) 20% piperidine, DMF; (d) $(Boc)_2O$, Et_3N, DCM; (e) HATU, DIPEA, DMF; (f) 20% TFA, DCM.

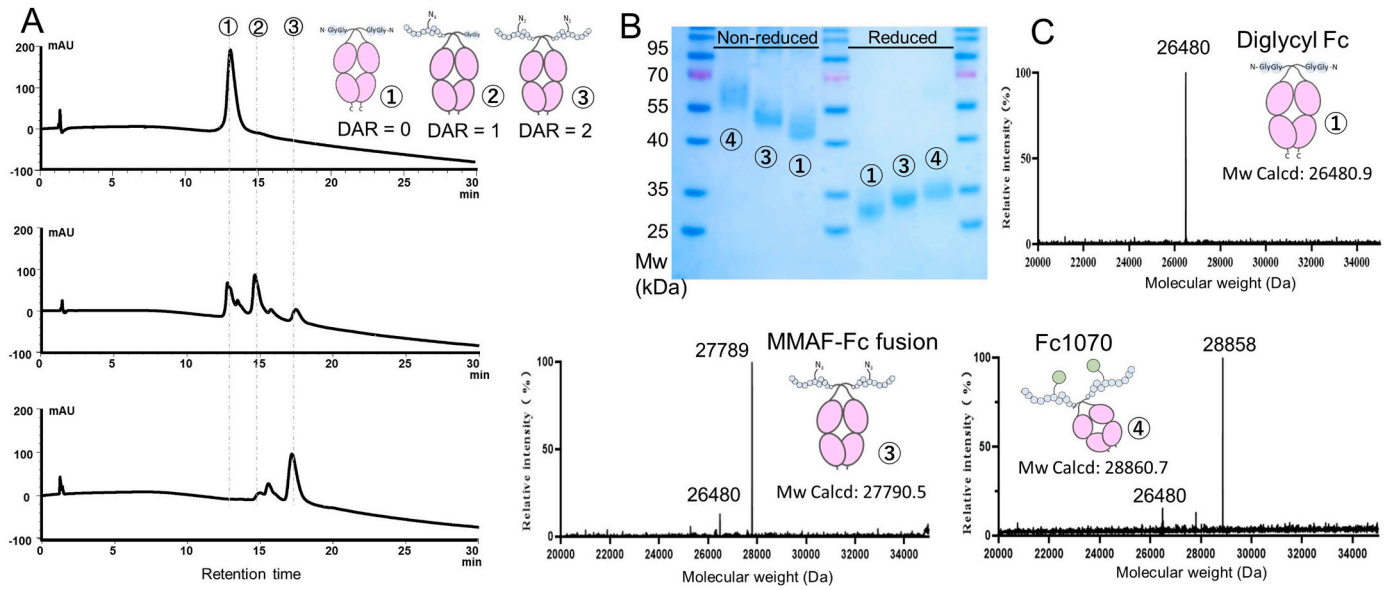

Fig. 1. Molecular characterization of Fc1070 and its precursors. (A) HIC chromatograms of DAR species under Sortase-A ligation conditions. Transpeptidation reactions were titrated at pseudopeptide-1441/Fc protein molar ratio of 0/1 (upper), 3/1 (middle) and 10/1 (bottom), respectively. (B) SDS-PAGE analysis of Fc1070 and its precursors to confirm the molecular weight and homodimer state. (C) Deconvoluted mass spectra of Fc1070 and its precursors under the reducing condition. The Mw calcd is based on the monomer chain because of the reducing condition.

2.3. In vitro and in vivo trafficking

To track the internalized drugs, LNCaP cells were treated with sulfo-Cy5 labelled bioconjugates and imaged by confocal microscopy (Fig. 3A). Observation after 30 min treatment showed that both SMDC1070 and Fc1070 were associated with the cell membrane. However, the distribution on membrane was punctuated and clustered along the cell boundary, suggesting that the PSMA-SMDC complex has already migrated to the curvature of clathrin-coated pits and been undergoing a local envelopment [29]. As the incubation time increases, they were internalized and mounted up to a level that could be co-localized with Lysotracker Green (Fig. S3). At the 3h timepoint, the intracellular accumulation in LNCaP cells was pronounced and majority of SMDC has been transported into endosome/lysosome vesicles. By comparing the intracellular distribution pattern between Fc1070 and SMDC1070, we did not observe any aberrant difference in neither the binding capacity nor internalization rate, in spite of the fact that Fc1070 is almost 25 times larger than SMDC1070 in molecular mass. These results collectively suggested that Fc1070 can be internalized as efficient as SMDC by tumor cells, thus suitable for toxin delivery.

We then investigated the potential of Fc1070 to reach tumors in vivo. As showed in Fig. 3B, intravenous administration of near-infrared (NIR) fluorescent dye sulfo-Cy7 labelled Fc1070 resulted in visible tumor accumulation after 12 h, and the strong fluorescence persisted in LNCaP tumors for at least 48 h. By contrast, the fluorescence of tumors homed by SMDC1070 started to decline at 24 h timepoint, despites it remained visible 48 h after injection. The short retention of SMDC1070 in tumor is likely due to its lower binding affinity to PSMA receptor and faster clearance from systemic circulation. After intravenous administration, SMDC1070 were barely accumulated in heart, lungs and spleen, instead vastly visible at kidneys. Indeed, NIR imaging of the dissected organs and tumors revealed that the fluorescence was restricted to PSMA positive tumors and excretory organ kidneys. In comparison to the quick elimination of SMDC1070 by the kidney, Fc1070 was metabolized mainly via liver, a typical biodistribution pattern also exhibited by antibodies [30]. Since Fc1070 shares same targeting ligand with SMDC1070, these results suggested that the Fc protein dominates the profound tumor deposition and in vivo pro-liver trafficking profile of the bioconjugate.

2.4. Prolonged blood circulation and organ allocation

The antibody-like trafficking performance of Fc1070 motivated us to investigate the blood retention time in mice. Three groups of mice were intravenously injected with equivalent doses of sulfo-Cy7 labelled Fc1070, SMDC1070 and human antibody IgG, respectively. The blood was collected at indicated timepoints and analyzed by the Odyssey infrared scanner. The persistent strong fluorescence was observed throughout the experiment within the blood samples of both IgG and Fc1070 groups whereas fluorescence signals in SMDC1070 group quickly decayed away in hours (Fig. 3C). Quantitative analysis showed that SMDC1070 was eliminated from blood quickly and exhibits a half-life as short as 0.5 h. In contrast, Fc1070 has a similar pharmacokinetic profile to IgG, with a circulating half-life of 79 h (Fig. 3C and Fig. S4). This feature positioned SMDC-Fc bioconjugate as an ideal platform for long-term drug delivery, in particular as a competitor to ADC.

The prolonged blood circulation of Fc1070 in vivo was mediated by the Fc domain. It not only rescues Fc1070 from endothelial pinocytosis by the FcRn recycling process but also restricts the renal clearance owing to its relatively bulky size [31]. In aspects of molecular weight, Fc1070 (57.7 kDa) is larger than SMDC1070 (2.5 kDa) but still quite smaller than a typical antibody (~ 150 kDa). Despite compact, its hydrodynamic size remains above the typical renal clearance threshold (50 kDa) and can support the long circulation in the blood stream. This claim was evidenced by the FDA-approved Dulaglutide, a 59.7 kDa Fc fusion protein showing a biological half-life of approximately 4.7 days [32]. Fluorescent images of organ sections in Fig. 3D revealed the relative liver-to-kidney distribution of Fc1070 and SMDC1070. Due to the threshold effect, Fc1070 was partially spotted in kidney, but the magnitude of drug deposition was substantially higher in liver, likely due to the high congestion of liver. A reverse distribution relationship was revealed by SMDC1070, which reinforces the important role of Fc domain in organ allocation.

The bulky size after Fc grafting raised the concern of tumor penetration efficiency, since the larger size is reluctant to infiltrate the tumor [33]. To elucidate this, fluorescently tagged IgG, Fc1070 and SMDC1070 were incubated with the 22RV1 tumors and the tissue infiltration was visualized by tumor section scanning. After inspection of the penetration depth, it was found that Fc1070 infiltrated the tumor tissues with an

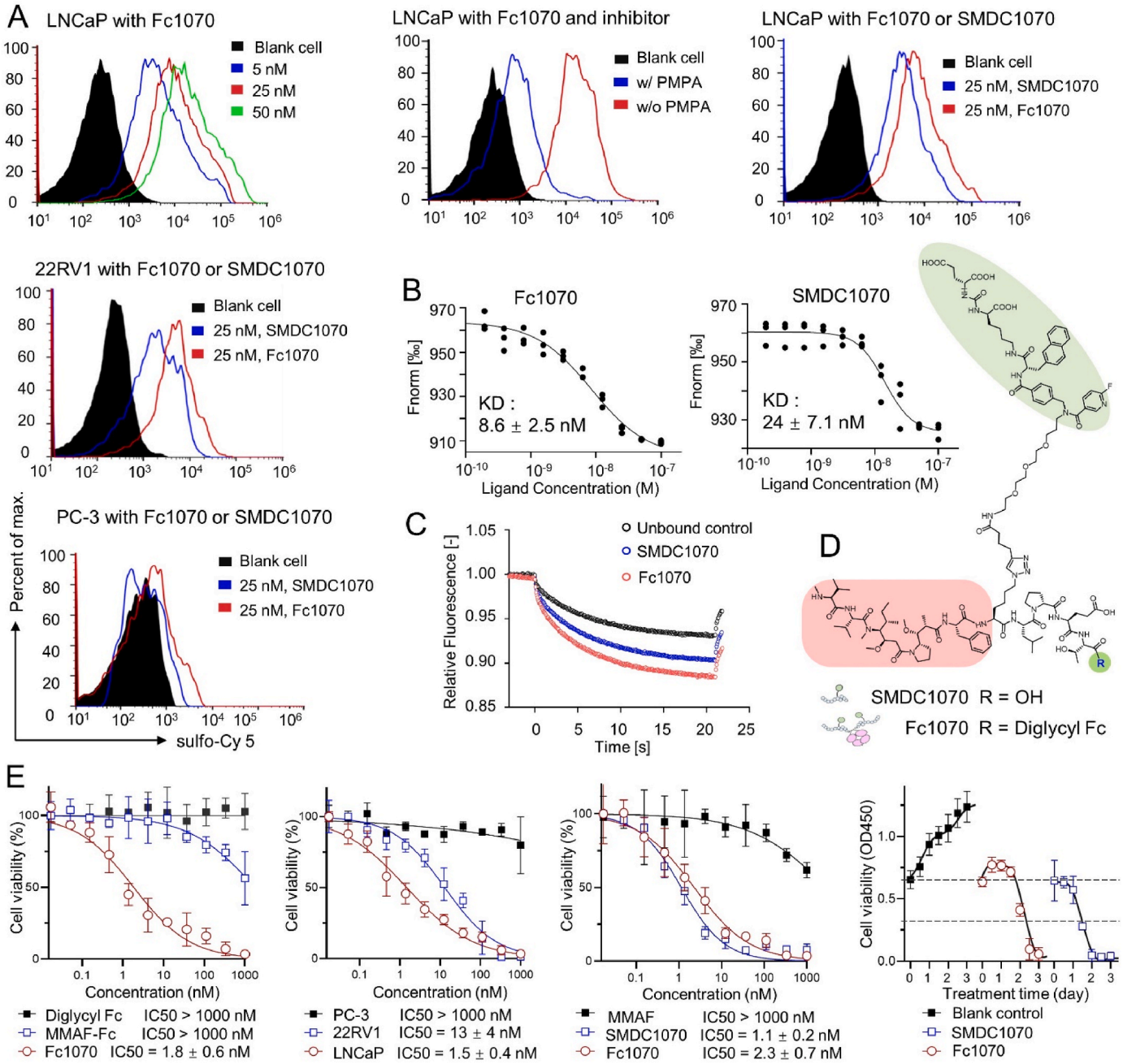

Fig. 2. The selectivity and potency of Fc1070 to the PSMA positive cancer cells. (A) Flow cytometry analysis revealing dose-dependent and selective binding of Fc1070 to LNCaP cells. The binding strength to 22RV1 and PC-3 cells is lower, but well correlated with their PSMA expression patterns. (B) Affinity profiling of Fc1070 and SMDC1070 to PSMA by MST KD test (n = 3). (C) MST trace of Fc1070 against PSMA showing a deeper shift in magnitude than that of SMDC1070. (D) Chemical structures of Fc1070 and its counterpart SMDC1070. DUPA ligand and MMAF are highlighted by blue grey and pink, respectively. (E) Cytotoxicity of Fc1070 and SMDC1070 on prostate cancer cell lines. The Fc1070 is much more potent than the ligand-free MMAF1070 and drug-free Fc on PSMA-positive LNCaP cells (left panel). The PSMA expression status also has apparent impact on the bioactivity of Fc1070 (middle left), reflecting the selectivity of cytotoxicity. Compared to SMDC1070, Fc1070 has a slightly lower potency (middle right) and slower cell response (right panel). Data are shown as mean ± SD (n = 3). (For interpretation of the references to colour in this figure legend, the reader is referred to the Web version of this article.)

efficacy less prominent than SMDC1070 but remarkably deeper than IgG (Fig. 3E). As was to be expected, the compact size of SMDC-Fc can have an advantage in context of tumor penetration compared with the large-format ADC that use two Fab domains fused to Fc for tumor targeting.

2.5. *In vivo therapy and ligands switch for generality*

Therapeutic evaluation of Fc1070 and SMDC1070 was performed at equivalent doses of cytotoxic MMAF in nude mice bearing 22RV1 tumors. This tumor cell line displays a smaller cell surface density of PSMA receptors compared to LNCaP but is more convenient for inoculation and tumorigenesis [34]. In contrast to the rapid tumor growth in mice treated with saline, Fc1070 almost eliminated the tumors after a single dosing of 7 mg/kg at day 10, although a regrowth occurred three weeks later (Fig. 4B). In lowering the dose to 1 mg/kg, efficacy of Fc1070 dropped off, but still demonstrated a profound anti-tumor growth effect. Single administration of SMDC1070 at dose of 240 nmol/kg (MMAF

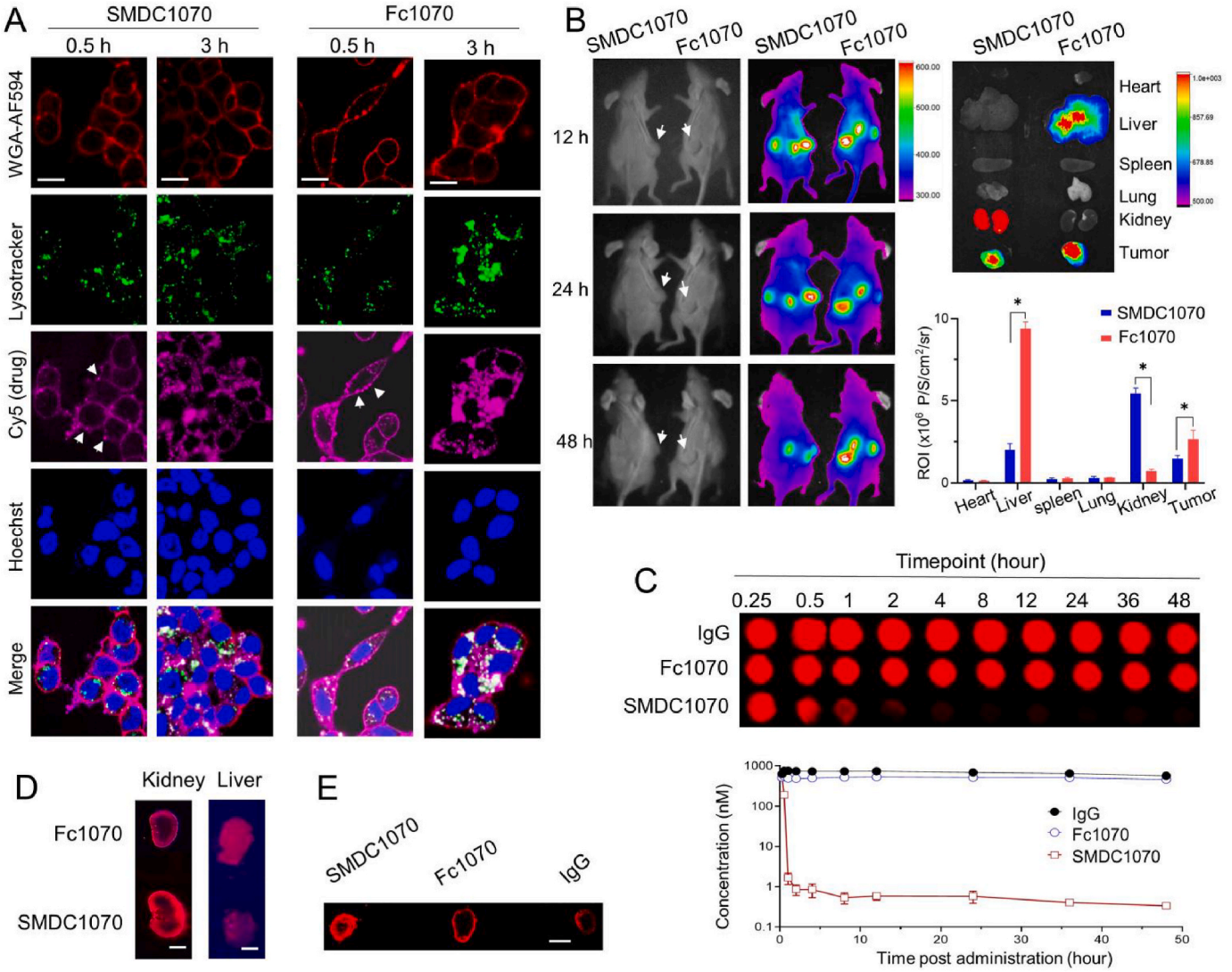

Fig. 3. In vitro and in vivo tracking of Fc1070 and its counterpart SMDC1070. (A) Confocal microscopy images of PSMA positive LNCaP cells after exposure to sulfo-Cy5 labelled SMDC1070 (left panel) and Fc1070 (right panel) for different time intervals. Arrow indicates the clusters on cell membrane. Scar bar: 20 μm. WGA-AF594, Alexa Fluor 594 labelled wheat germ agglutinin for plasma membrane staining; Lysotracker, lysotracker green to counterstain the endosome/lysosomes; Hoechst, Hoechst 33342 for nuclear staining. (B) In vivo trafficking of Fc1070 and SMDC1070 in mice bearing LNCaP xenografts. Arrows indicate the tumor sites. $^*P < 0.05$, data are shown as mean ± SD (n = 3). (C) Blood pharmacokinetics of sulfo-Cy7 labelled IgG, Fc1070 and SMDC1070 after single administration of equal doses. Data are shown as mean ± SD (n = 3). (D) Representative fluorescence images of kidney and liver sections from mice injected intravenously with sulfo-Cy7 labelled Fc1070 and SMDC1070. Red, sulfo-Cy7; blue, nuclei counterstained by TO-PRO-3. Scar bar, 2.5 mm. (E) Section images of tumors infiltrated by sulfo-Cy7 labelled IgG, Fc1070 and SMDC1070 for 4 h at room temperature. Red, sulfo-Cy7. Scar bar, 5 mm. (For interpretation of the references to colour in this figure legend, the reader is referred to the Web version of this article.)

equivalent to 7 mg/kg of Fc1070, DAR = 2) only lead to a weak retardation of tumor growth. This result is reasonable considering its extremely short half-life period in blood circulation and the limited on-target exposure of SMDC1070 after single dosing. It was expected that the repeat-dose administration would allow continuous blood exposure of SMDC to targets and might lead to a better anti-tumor efficacy. In a parallel study, we did observe the tumor growth slowdown by SMDC1070 with a dosing regimen of 240 nmol/kg every 5 days up to 4 doses (Fig. S5). No body weight decrease was observed in all the groups during the treatment time, showing the safety of bioconjugates (Fig. S6). Additional toxicity evaluations such as the apoptosis and histochemical staining further confirm the absence of in vivo toxicity (Fig. S7 and Fig. S8).

In this study, of particular interest is the on-demand use of the SMDC-Fc platform to confront tumors of different markers. The high-throughput generation of the bioconjugates can be achieved by switching the small-molecule ligands from the predefined toolbox using the CuAAC chemistry (Fig. 4A). Under our optimized miniature reaction, the SMDC-Fc can be synthesized at room temperature and cleaned up by a simple desalting step with almost quantitative yield in 2 h. The proof of concept was demonstrated by installing folate receptor (FR) ligand folic acid (FA) and carbonic anhydrase IX (CAIX) receptor ligand acetazolamide (AZA) on Fc to treat the KB tumor and SKRC-52 tumor, respectively. As shown in Fig. 4B, the FR specific Fc606, both in high dose (7 mg/kg) and low dose (1 mg/kg), exhibited the excellent anti-tumor discrimination relative to the counterpart SMDC606 and saline control. However, the therapeutic activity of Fc274 that targets to CAIX receptors, was inferior to its peers Fc1070 and Fc606. This observation was somehow unexpected because the NIR in vivo trafficking study indicated that SKRC-52 tumor was well targeted and deposited by Fc274 in mice (Fig. S9). It was also unlikely relevant to the penetrating disparity, in light of the poor response of SKRC-52 tumor to the repeat

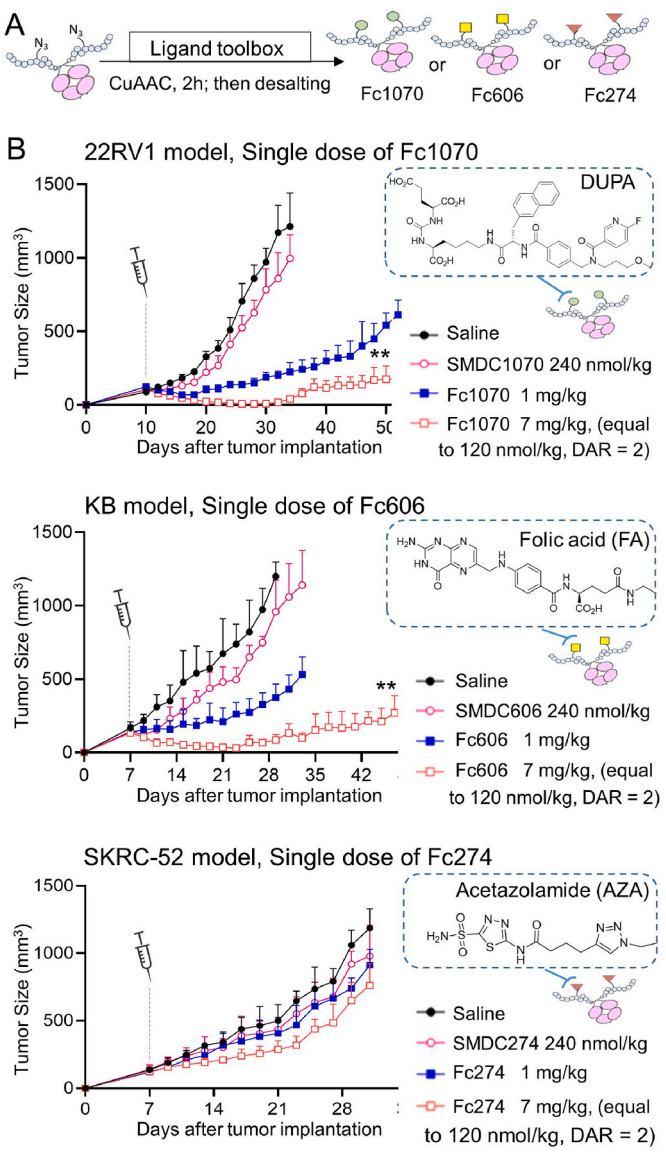

Fig. 4. In vivo antitumor efficacy in xenograft models. (A) Schematic diagram showing the fast generation of SMDC-Fc for in vivo therapy by CuAAC click chemistry. (B) Growth of xenografts in balb/c nude mice treated with single injection of the corresponding SMDC, SMDC-Fc or saline control. Both conjugates were administrated at doses of equimolar amounts of MMAF (240 nmol/kg). A low-dose regimen of SMDC-Fc (1 mg/kg) was evaluated in parallel. The core structures of small-molecule ligands were boxed as indicated, and full structures were available in Fig. S11. Data are shown as mean ± SD (n = 5–6). $^{**}P \leq 0.01$.

injections of SMDC274 (Fig. S5). In vitro profiling of drug cytotoxicity also showed that both Fc274 and SMDC274 were poor cell-killers in spite of their strong binding to SKRC-52 cells (Fig. S10). These observations can be explained by results from previous reports that an acetazolamide-based ligand is a high-affinity CAIX binder but lacks of efficient internalization capability [35,36]. Precaution of the linker-payload choice is essential to the therapeutic performance of acetazolamide guided chemotherapy, as the payloads have to be released outside and permeate into cells for killing [5]. Collectively, these results demonstrated that receptor mediated internalization is essential to unfold the cytotoxic potential of SMDC-Fc and CAIX receptor ligands might not fit this platform.

3. Conclusion

SMDC shows great promise for targeted cancer chemotherapy, but there application is hampered by a short blood retention time in vivo. Here, we present an approach that shows considerable promise in the attempt to overcome this shortcoming. In this practice, Fc protein can be cheaply produced in bacteria expression system and easily grafted with drug by enzymatic ligation. Compared to the full-length antibody produced in mammalian hosts, the Fc protein in the study can be easily expressed and well folded in the cytoplasm of T7 Shuffle bacteria strain. Using a two-day culture process and a rapid Ni-NTA affinity chromatography, it was possible to purify nearly 100 mg of His tag Fc protein from shake flasks holding 1 L of culture in our lab. It was expected that scale-up from shake flasks to industrial bioreactor would easily surpass the yield of 1 g/L at a tremendous low cost.

Focusing on prostate cancer therapy, a small-molecule ligand of DUPA was chosen from the ligand toolbox and installed onto Fc to emulate a PSMA specific ADC. Subsequent in vitro and in vivo characterization showed that the bioconjugate achieves the low nanomolar KD value, specific recognition to tumor cells, efficient cellular internalization, long-term circulation, high deposition at tumor site and profound anti-tumor effect, which meet the most key parameters of the bench-to-clinic ADCs. In addition, the proposed small-molecule ligand-based SMDC approach, as opposed to the conventional ADC using complex Fab domains for targeting, offers an impressive thermal stability (Fig. S12), thus may help to prolong the shelf life of the bioconugate.

Another important consideration is the adaptable ligand switch for fast generation of new SMDC-Fc to intervene on different cancer types, which has proven to be feasible in this study. Compared to antibody screening, isolation of small organic ligands is more difficult. So far, the validated small-molecule ligands are limited to a small number of tumor targets. Nevertheless, the DNA-encoded chemical library technology has been emerging as powerful tool to discover small-molecules inhibitors against target proteins in the pharmaceutical industry [37]. By expanding the concept to the tumor-targeting ligand discovery, it may enable the fast screening of small-molecule ligands to any tumor targets of interest [38]. Overall, the Fc grafted SMDC technology reported here represents a highly modular and effective platform that may have potential application in targeted cancer chemotherapy.

4. Materials and methods

4.1. Cell culture

LNCaP, 22RV1, SKRC-52, KB and PC-3 cells were purchased from American Type Culture Collection (ATCC). Upon thaw, LNCaP, 22RV1 and SKRC-52 cells were cultured in Roswell Park Memorial Institute 1640 medium (RPMI 1640, Gibco) supplemented with 10% fetal bovine serum (FBS, Gibco) and 1% penicillin-streptomycin (PS, Gibco). KB cells were cultured in folate-free RPMI 1640 (Thermo Fisher) supplemented with 10% FBS and 1% PS. PC-3 cells were cultured in Dulbecco's Modified Eagle Medium (DMEM, Gibco) supplemented with 10% FBS and 1% PS. All cells were maintained in a humidified cell culture incubator at 37 °C with 5% carbon dioxide (CO_2).

4.2. Protein expression, conjugation and purification

pET-28a/IgG_1 Fc-His tag was constructed by PCR cloning the cDNA of cetuximab's Fc domain into a pET-28a vector. To generate the N-terminal diglycyl Fc, a Sortase A substrate peptide sequences (LPETGG) was fused to the Fc's N-terminus. The corresponding cDNA of this substrate peptide was cloned into the above vector by Gibson assembly cloning. The vector was transformed into Shuffle T7 *E. coli* and the Fc protein expression was induced by the Studier autoinduction method [39]. Bacteria were harvested by centrifugation for 10 min at 8000 g, and lysed by French press homogenization. The soluble proteins were

collected and the Fc protein was purified by Ni-affinity chromatography. To obtain the diglycyl Fc, the His-tagged protein was site-specifically cleaved by Sortase A in the presence of triglycine. Briefly, the purified protein was diluted to 7.5 mg/ml in TBS buffer and coincubated with triglycine (1 mM) at room temperature for 6h in the presence of 300 nM of 7 M Sortase A (a calcium-independent Sortase A variant with increased activities) [40]. The product was precipitated by 85% ammonium sulfate solution, and desalted with G-25 column (GE Life Sciences) to remove small molecules such as triglycine and ammonium sulfate. The diglycyl Fc protein (5 mg/ml) was then mixed with pseudopeptide-1441 at molar ratio of 1/10 in the presence of 7 M Sortase A (200 nM) in TBS buffer (overnight at room temperature). The reaction was precipitated with ammonium sulfate and further desalted with G-25 column aforementioned to yield the MMAF-Fc fusion protein. The small-molecule ligand was installed onto the fusion protein by copper catalyzed cycloaddition (CuAAC) click reaction. Briefly, 3 mg/ml of MMAF-Fc fusion protein was mixed with alkyne functionalized targeting ligands (4 equiv) in PBS buffer containing 10% glycerol as protein stabilizer. The reaction was catalyzed by THPTA chelated Cu^{+} and incubated at room temperature for 2 h. The final product was purified by gel filtration chromatography (Superdex 200 HR 10/30 column, GE Life Sciences) using PBS as the elution buffer. All conjugation products were analyzed by SDS-PAGE and ESI-Q-TOF MS to confirm the purity and size. The purified products (SMDC-Fc) were concentrated by ultrafiltration and stored in PBS buffer containing 20% glycerol at −30 °C.

Protein Sequence of IgG_1 Fc with a 6xHis tag and LPETGG substrate peptide:

MGSSHHHHHHSSGLVPRGSHMASLPETGGGGG-
SEPKSSDKTHTCPPCPA-
PELLGGPSVFLFPPKPKDTLMISRTPEVTCVVVDV-
SHEDPEVKFNWYVDGVEVHNAKTKPREEQYN-
STYRVVSVLTVLHQDWLNGKEYKCKVSNKALPAPIEKTISKAKGQ-
PRE-
PQVYTLPPSREEMTKNQVSLTCLVKGFYPSDIAVE-
WESNGQPENNYKTTPPVLDSDGSF-
FLYSKLTVDKSRWQQGNVFSCSVMHEALHNHYTQKSLSLSPGK

4.3. HIC analysis

To optimize the drug-to-antibody ratio (DAR), the Sortase A-mediated transpeptidation reaction was monitored using SHIMADZU LC-40D HPLC system equipped with a Tosoh TSKgel Butyl-NPR hydrophobic interaction chromatography (HIC) column (4.6 × 100 mm, 5 μm, TOSOH Bioscience). Elution condition was as follows: mobile phase A = 25 mM sodium phosphate including 1.5 M ammonium sulfate (pH 7.0); mobile phase B = 25 mM sodium phosphate containing 20% isopropanol (pH 7.0); gradient over 30min from 0 to 100% B; flow rate = 0.5 ml/min. Average DAR values were determined by integration of peak areas.

4.4. Cell binding and flow cytometry analysis

To minimize the internalization upon receptor binding, all the experiments were performed at room temperature. Briefly, SMDC-Fc or SMDC (sulfo-Cy5 labelled) and cancer cells (~20000 cells) were incubated for 1 h in serum-free RPMI 1640 media supplemented with 1% BSA. The cells were washed twice with RPMI 1640 and analyzed on a BD LSR II flow cytometer (Beckton Dickinson).

4.5. Binding affinity assay

MicroScale Thermophoresis (MST) experiments were performed according to the manufacturer's protocol [41]. To profile the KD, serial dilutions of Fc1070, SMDC1070 and MMAF-Fc fusion (unbound control) in PBS buffer was titrated against a constant concentration of PSMA ECD that was genetically fused with a fluorescent protein mClover for signaling. Briefly, PSMA was diluted to the concentration of approximately 20 nM in PBS buffer. Then, 50 μl of diluted ligands was mixed with 50 μl of the PSMA solution (final concentration 10 nM). The mixture was incubated on ice for 15 min in the dark. The MST traces were recorded using the standard parameters.

4.6. Confocal imaging

The confocal laser scanning microscopy was utilized to locate the positions of SMDC-Fc or SMDC in cancer cells. Briefly, 25 nM of SMDC-Fc (sulfo-Cy5 labelled) and SMDC (sulfo-Cy5 labelled) were incubated with cancer cells (~5000 cells) at 37 °C for 0.5h, 1.5h and 3h, respectively. Endosomes and lysosomes were stained with Lyso Tracker® Green DND-26 (Invitrogen), nuclei were stained with Hoechst 33342, and cell membranes were stained with wheat germ agglutinin (WGA, Alexa Fluor 594 labelled). At predetermined intervals, cells were imaged by confocal laser scanning microscopy.

4.7. Cell viability

Cells (LNCaP, 22RV1, SKRC-52, KB and PC-3 cells) were seeded in a culture-treated 96-well clear plate (~3000 cells per well) and allowed to adhere overnight. Serial dilutions of drug were added to each well and incubated for 72 h. Cell viability was measured using the Cell Counting Kit-8 (CCK-8) according to the protocol. Briefly, 15 μl of CCK-8 solution was added into the culture. After the 2-h incubation at 37 °C, the absorbance at a wavelength of 450 nm was measured by a microplate reader (TECAN) and profiled for IC50 value.

4.8. Western blot

In order to examine the stability of SMDC-Fc, the protein integrity was examined by western blotting. Protein samples were separated by 4–20% SDS-PAGE and transformed to polyvinylidene fluoride (PVDF) (Amersham). After blocking in 1% BSA for 2 h at room temperature, the membranes were incubated with mouse anti-human IgG Fc antibody HRP conjugate for 2 h. After washing, the membrane was incubated with western detection kit (Cell Signaling Technologies) and imaged by ChemiDoc Imaging Systems (Bio-Rad).

4.9. In vivo biodistribution

All the animal studies were performed in compliance with the guidelines of the Chinese Regulations for the Administration of Affairs Concerning Experimental Animals and the Institutional Animal Care and Use Committee of Wuhan University. Trypsinized LNCaP or 22RV1 or SKRC-52 cells were washed twice with RPMI 1640 and resuspended in 1:1 mixture of RPMI 1640 (Gibco) and Matrigel (Corning). Cells (5×10^6) were injected subcutaneously into the dorsa of 6-8-week-old male BALB/c-nu mice. Tumor growth was measured 3 times per week and size was calculated using the formula length × $width^2/2$. The biodistribution study was performed when the tumor volume reached 400–600 mm^3. SMDC-Fc (sulfo-Cy7 labelled, 5 mg/kg) and SMDC (sulfo-Cy7 labelled, equal dye dose) were injected into mice via the tail vein in a volume of 150 μl. Mice were then imaged using the IVIS in vivo imaging system (Bruker Xtreme BI) at 12, 24, and 48 h. At the end of the experiment, the mice were euthanized. The tumors and major organs (heart, lung, liver, spleen, and kidney) were harvested and imaged. Tissues were frozen later for section analysis.

4.10. Pharmacokinetic studies

For pharmacokinetic studies, C57/BL6 mice were intravenously injected with either SMDC-Fc (sulfo-Cy7 labelled, 5 mg/kg) or SMDC (sulfo-Cy7 labelled, equal dye dose). Approximately 30 μl of blood was obtained at 0.25, 0.5, 1, 2, 4, 8, 10, 12, 24, 36 and 48 h after injection. Blood samples were imaged and quantified using an Odyssey CLx

imaging system (LI-COR Biosciences).

4.11. In vivo therapy

To minimize the impact of diet on serum folate levels, all mice for KB exnograft model were fed with folic acid deficient diet 4 weeks ahead of tumor implantation, and maintained throughout the experiments [42]. The other groups were fed normally. For inoculation, trypsinized 22RV1 or SKRC-52 or KB cells were washed twice with RPMI 1640 and suspended in 1:1 mixture of RPMI 1640 (Gibco) and Matrigel (Corning). Cell suspension (200 μl, 5 million cells) were injected subcutaneously into the dorsa of 6-8-week-old male BALB/c-nu mice. When tumor sizes reached about 100 mm^3, SMDC-Fc and SMDC were administered as the dosage regimen recommended. Body weight and tumor size were measured every 2 days. Mice were euthanized once tumor size exceeded 1000 mm^3.

4.12. Statistical analysis

The mean ± standard deviation (SD) was used to report all data. A GraphPad Prism software was used to conduct statistical comparisons using the student's *t*-test as $^*P < 0.05$, $^{**}P < 0.01$. A difference of $^*P < 0.05$ was considered significant.

Credit author statement

Yan Zheng: Conceptualization, Methodology, Investigation, Writing-Original draft preparation, Ruolin Xu.: Investigation, Validation, Siyi Chen: Visualization, Wanyi Tai: Conceptualization, Supervision and Writing – Review & Editing.

Declaration of competing interest

The authors declare that they have no known competing financial interests or personal relationships that could have appeared to influence the work reported in this paper.

Data availability

Data will be made available on request.

Acknowledgements

This work was financially supported by the National Key R&D Program of China (Grant No. 2021YFA0909900) and the National Natural Science Foundation of China (Grant No. 82073770).

Appendix A. Supplementary data

Supplementary data to this article can be found online at https://doi.org/10.1016/j.biomaterials.2022.121820.

References

[1] Z. Zhao, A. Ukidve, J. Kim, S. Mitragotri, Targeting strategies for tissue-specific drug delivery, Cell 181 (1) (2020) 151–167.
[2] C. do Pazo, K. Nawaz, R.M. Webster, The oncology market for antibody-drug conjugates, Nat. Rev. Drug Discov. 20 (8) (2021) 583–584.
[3] C.P. Leamon, J.A. Reddy, A. Bloomfield, R. Dorton, M. Nelson, M. Vetzel, P. Kleindl, S. Hahn, K. Wang, I.R. Vlahov, Prostate-specific membrane antigen-specific antitumor activity of a self-immolative tubulysin conjugate, Bioconjugate Chem. 30 (6) (2019) 1805–1813.
[4] J.A. Reddy, R. Dorton, E. Westrick, A. Dawson, T. Smith, L.C. Xu, M. Vetzel, P. Kleindl, I.R. Vlahov, C.P. Leamon, Preclinical evaluation of EC145, a folate-vinca alkaloid conjugate, Cancer Res. 67 (9) (2007) 4434–4442.
[5] N. Krall, F. Pretto, W. Decurtins, G.J. Bernardes, C.T. Supuran, D. Neri, A small-molecule drug conjugate for the treatment of carbonic anhydrase IX expressing tumors, Angew. Chem., Int. Ed. Engl. 53 (16) (2014) 4231–4235.
[6] M. Wichert, N. Krall, W. Decurtins, R.M. Franzini, F. Pretto, P. Schneider, D. Neri, J. Scheuermann, Dual-display of small molecules enables the discovery of ligand pairs and facilitates affinity maturation, Nat. Chem. 7 (3) (2015) 241–249.
[7] S. Cazzamalli, A. Dal Corso, F. Widmayer, D. Neri, Chemically defined antibody- and small molecule-drug conjugates for in vivo tumor targeting applications: a comparative analysis, J. Am. Chem. Soc. 140 (5) (2018) 1617–1621.
[8] P. Khongorzul, C.J. Ling, F.U. Khan, A.U. Ihsan, J. Zhang, Antibody-drug conjugates: a comprehensive review, Mol. Cancer Res. 18 (1) (2020) 3–19.
[9] D.Y. Jackson, Processes for constructing homogeneous antibody drug conjugates, Org. Process Res. Dev. 20 (5) (2016) 852–866.
[10] V. Oganesyan, M.M. Damschroder, K.E. Cook, Q. Li, C. Gao, H. Wu, W. F. Dall'Acqua, Structural insights into neonatal Fc receptor-based recycling mechanisms, J. Biol. Chem. 289 (11) (2014) 7812–7824.
[11] T. Suzuki, A. Ishii-Watabe, M. Tada, T. Kobayashi, T. Kanayasu-Toyoda, T. Kawanishi, T. Yamaguchi, Importance of neonatal FcR in regulating the serum half-life of therapeutic proteins containing the Fc domain of human IgG1: a comparative study of the affinity of monoclonal antibodies and Fc-fusion proteins to human neonatal FcR, J. Immunol. 184 (4) (2010) 1968–1976.
[12] D. Levin, B. Golding, S.E. Strome, Z.E. Sauna, Fc fusion as a platform technology: potential for modulating immunogenicity, Trends Biotechnol. 33 (1) (2015) 27–34.
[13] A. Beck, J.M. Reichert, Therapeutic Fc-fusion proteins and peptides as successful alternatives to antibodies, mAbs 3 (5) (2011) 415–416.
[14] F. Gallo, B. Korsak, C. Müller, T. Hechler, D. Yanakieva, O. Avrutina, H. Kolmar, A. Pahl, Enhancing the pharmacokinetics and antitumor activity of an α-amanitin-based small-molecule drug conjugate via conjugation with an Fc domain, J. Med. Chem. 64 (7) (2021) 4117–4129.
[15] L. Jendeberg, P. Nilsson, A. Larsson, P. Denker, M. Uhlén, B. Nilsson, P.A. Nygren, Engineering of Fc(1) and Fc(3) from human immunoglobulin G to analyse subclass specificity for staphylococcal protein A, J. Immunol. Methods 201 (1) (1997) 25–34.
[16] H. Donaghy, Effects of antibody, drug and linker on the preclinical and clinical toxicities of antibody-drug conjugates, mAbs 8 (4) (2016) 659–671.
[17] G.I. Shapiro, U.N. Vaishampayan, P. LoRusso, J. Barton, S. Hua, S.D. Reich, R. Shazer, C.T. Taylor, D. Xuan, H. Borghaei, First-in-human trial of an anti-5T4 antibody-monomethylauristatin conjugate, PF-06263507, in patients with advanced solid tumors, Invest. N. Drugs 35 (3) (2017) 315–323.
[18] L. Pan, W. Zhao, J. Lai, D. Ding, Q. Zhang, X. Yang, M. Huang, S. Jin, Y. Xu, S. Zeng, J.J. Chou, S. Chen, Sortase A-generated highly potent anti-CD20-MMAE conjugates for efficient elimination of B-lineage lymphomas, Small 13 (6) (2017), 201602267.
[19] S. Dickgiesser, N. Rasche, D. Nasu, S. Middel, S. Hörner, O. Avrutina, U. Diederichsen, H. Kolmar, Self-assembled hybrid aptamer-fc conjugates for targeted delivery: a modular chemoenzymatic approach, ACS Chem. Biol. 10 (9) (2015) 2158–2165.
[20] S.O. Doronina, T.D. Bovee, D.W. Meyer, J.B. Miyamoto, M.E. Anderson, C. A. Morris-Tilden, P.D. Senter, Novel peptide linkers for highly potent antibody-auristatin conjugate, Bioconjugate Chem. 19 (10) (2008) 1960–1963.
[21] S.C. Alley, D.R. Benjamin, S.C. Jeffrey, N.M. Okeley, D.L. Meyer, R.J. Sanderson, P. D. Senter, Contribution of linker stability to the activities of anticancer immunoconjugates, Bioconjugate Chem. 19 (3) (2008) 759–765.
[22] D.J. Williamson, M.E. Webb, W.B. Turnbull, Depsipeptide substrates for sortase-mediated N-terminal protein ligation, Nat. Protoc. 9 (2) (2014) 253–262.
[23] J. Cardinale, M. Roscher, M. Schäfer, M. Geerlings, M. Benešová, U. Bauder-Wüst, Y. Remde, M. Eder, Z. Nováková, L. Motlová, C. Barinka, F.L. Giesel, K. Kopka, Development of PSMA-1007-related series of (18)F-labeled glu-ureido-type PSMA inhibitors, J. Med. Chem. 63 (19) (2020) 10897–10907.
[24] J. Cardinale, M. Schäfer, M. Benešová, U. Bauder-Wüst, K. Leotta, M. Eder, O. C. Neels, U. Haberkorn, F.L. Giesel, K. Kopka, Preclinical evaluation of (18)F-PSMA-1007, a new prostate-specific membrane antigen ligand for prostate cancer imaging, J. Nucl. Med. 58 (3) (2017) 425–431.
[25] A. Juzeniene, V.Y. Stenberg, S. Bruland Ø, R.H. Larsen, Preclinical and clinical status of PSMA-targeted alpha therapy for metastatic castration-resistant prostate cancer, Cancers 13 (4) (2021).
[26] S.A. Kularatne, K. Wang, H.K. Santhapuram, P.S. Low, Prostate-specific membrane antigen targeted imaging and therapy of prostate cancer using a PSMA inhibitor as a homing ligand, Mol. Pharm. 6 (3) (2009) 780–789.
[27] M. Sahin, M.M. Remy, B. Fallet, R. Sommerstein, M. Florova, A. Langner, K. Klausz, T. Straub, M. Kreutzfeldt, I. Wagner, C.T. Schmidt, P. Malinge, G. Magistrelli, S. Izui, H. Pircher, J.S. Verbeek, D. Merkler, M. Peipp, D.D. Pinschewer, Antibody bivalency improves antiviral efficacy by inhibiting virion release independently of Fc gamma receptors, Cell Rep. 38 (5) (2022), 110303.
[28] I. Krop, E.P. Winer, Trastuzumab emtansine: a novel antibody-drug conjugate for HER2-positive breast cancer, Clin. Cancer Res. 20 (1) (2014) 15–20.
[29] W. Chen, D. ten Berge, J. Brown, S. Ahn, L.A. Hu, W.E. Miller, M.G. Caron, L. S. Barak, R. Nusse, R.J. Lefkowitz, Dishevelled 2 recruits beta-arrestin 2 to mediate Wnt5A-stimulated endocytosis of Frizzled 4, Science 301 (5638) (2003) 1391–1394.
[30] A. Giddabasappa, V.R. Gupta, R. Norberg, P. Gupta, M.E. Spilker, J. Wentland, B. Rago, J. Eswaraka, M. Leal, P. Sapra, Biodistribution and targeting of anti-5T4 antibody-drug conjugate using fluorescence molecular tomography, Mol. Cancer Therapeut. 15 (10) (2016) 2530–2540.
[31] T. Yamaoka, Y. Tabata, Y. Ikada, Body distribution of intravenously administered gelatin with different molecular weights, J. Contr. Release 31 (1) (1994) 1–8.
[32] J. Jendle, G. Grunberger, T. Blevins, F. Giorgino, R.T. Hietpas, F.T. Botros, Efficacy and safety of dulaglutide in the treatment of type 2 diabetes: a comprehensive

review of the dulaglutide clinical data focusing on the AWARD phase 3 clinical trial program, Diabetes Metab. Res. Rev. 32 (8) (2016) 776–790.
[33] A.I. Minchinton, I.F. Tannock, Drug penetration in solid tumours, Nat. Rev. Cancer 6 (8) (2006) 583–592.
[34] M. Kawada, H. Inoue, I. Usami, K. Takamoto, T. Masuda, Y. Yamazaki, D. Ikeda, Establishment of a highly tumorigenic LNCaP cell line having inflammatory cytokine resistance, Cancer Lett. 242 (1) (2006) 46–52.
[35] P.C. Lv, K.S. Putt, P.S. Low, Evaluation of nonpeptidic ligand conjugates for SPECT imaging of hypoxic and carbonic anhydrase IX-expressing cancers, Bioconjugate Chem. 27 (7) (2016) 1762–1769.
[36] S. Cazzamalli, A. Dal Corso, D. Neri, Acetazolamide serves as selective delivery vehicle for dipeptide-linked drugs to renal cell carcinoma, Mol. Cancer Therapeut. 15 (12) (2016) 2926–2935.
[37] G. Zimmermann, D. Neri, DNA-encoded chemical libraries: foundations and applications in lead discovery, Drug Discov, Today Off. 21 (11) (2016) 1828–1834.
[38] N. Favalli, G. Bassi, C. Pellegrino, J. Millul, R. De Luca, S. Cazzamalli, S. Yang, A. Trenner, N.L. Mozaffari, R. Myburgh, M. Moroglu, S.J. Conway, A.A. Sartori, M. G. Manz, R.A. Lerner, P.K. Vogt, J. Scheuermann, D. Neri, Stereo- and regiodefined DNA-encoded chemical libraries enable efficient tumour-targeting applications, Nat. Chem. 13 (6) (2021) 540–548.
[39] F.W. Studier, Protein production by auto-induction in high density shaking cultures, Protein, Expr. Purif. 41 (1) (2005) 207–234.
[40] H.J. Jeong, G.C. Abhiraman, C.M. Story, J.R. Ingram, S.K. Dougan, Generation of Ca2+-independent sortase A mutants with enhanced activity for protein and cell surface labeling, PLoS One 12 (12) (2017), e0189068.
[41] M. Jerabek-Willemsen, T. André, R. Wanner, H.M. Roth, S. Duhr, P. Baaske, D. Breitsprecher, MicroScale Thermophoresis: interaction analysis and beyond, J. Mol. Struct. 1077 (2014) 101–113.
[42] C.P. Leamon, J.A. Reddy, R. Dorton, A. Bloomfield, K. Emsweller, N. Parker, E. Westrick, Impact of high and low folate diets on tissue folate receptor levels and antitumor responses toward folate-drug conjugates, J. Pharmacol. Exp. Therapeut. 327 (3) (2008) 918–925.